Neuron, Vol. 32, 1149–1164, December 20, 2001, Copyright ©2001 by Cell Press

Rate, Timing, and Cooperativity Jointly Determine Cortical Synaptic Plasticity

Per Jesper Sjöström, Gina G. Turrigiano, and Sacha B. Nelson[1]
Brandeis University
Department of Biology
Volen Center for Complex Systems
Mailstop 008 415 South Street
Waltham, Massachusetts 02454

Summary

Cortical long-term plasticity depends on firing rate, spike timing, and cooperativity among inputs, but how these factors interact during realistic patterns of activity is unknown. Here we monitored plasticity while systematically varying the rate, spike timing, and number of coincident afferents. These experiments demonstrate a novel form of cooperativity operating even when postsynaptic firing is evoked by current injection, and reveal a complex dependence of LTP and LTD on rate and timing. Based on these data, we constructed and tested three quantitative models of cortical plasticity. One of these models, in which spike-timing relationships causing LTP "win" out over those favoring LTD, closely fits the data and accurately predicts the build-up of plasticity during random firing. This provides a quantitative framework for predicting the impact of in vivo firing patterns on synaptic strength.

Introduction

Prior studies have demonstrated that the induction of long-term potentiation (LTP) and depression (LTD) at neocortical and hippocampal synapses depend on the rate of afferent stimulation (Kirkwood et al., 1993), the number of afferents stimulated (Barrionuevo and Brown, 1983; Kirkwood and Bear, 1994), and the precise timing of this stimulation (Bi and Poo, 1998; Markram et al., 1997b). Nearly all of these studies have varied a single parameter, such as frequency, while keeping other parameters, such as timing and number of afferents stimulated, constant. In vivo, cortical neurons fire irregularly over a wide range of instantaneous frequencies (Shadlen and Newsome, 1998). Moreover, the precise timing of correlated firing between synaptically connected neurons can vary significantly (Gray, 1999). In order to predict how in vivo firing patterns influence long-term synaptic strength, it is crucial to develop a quantitative description of how the induction of plasticity depends jointly upon the rate, timing, and strength of a group of stimulated afferents. Here we have developed such a description for synapses between thick, tufted layer 5 (L5) pyramidal neurons in visual cortex.

Classical studies of LTP (Bliss and Lømo, 1973) and later LTD (Dudek and Bear, 1992; Mulkey and Malenka, 1992) emphasized the importance of firing rate in determining the sign and magnitude of synaptic plasticity. LTP is induced when afferents are stimulated at high rates, while lower rates of activity produce LTD (Dudek and Bear, 1992; Kirkwood et al., 1993; Mulkey and Malenka, 1992). Mechanistically, the rate dependence has been presumed to reflect the dependence of plasticity on postsynaptic calcium levels. High stimulation rates produce strong, rapid elevations in postsynaptic calcium required to induce LTP; lower stimulation rates produce more modest and/or slower elevations in postsynaptic calcium and as a result produce LTD (Bliss and Collingridge, 1993; Lisman, 1989; Yang et al., 1999).

Some early studies (Debanne et al., 1994; Gustafsson et al., 1987; Levy and Steward, 1983), and a larger number of recent studies found that the sign and magnitude of plasticity also depend critically on the precise timing of pre- and postsynaptic firing (Bi and Poo, 1998; Debanne et al., 1998; Egger et al., 1999; Feldman, 2000; Markram et al., 1997b; Zhang et al., 1998), a phenomenon termed spike timing-dependent plasticity (STDP) (Abbott and Nelson, 2000). At excitatory synapses onto cortical and hippocampal pyramidal neurons, pre-before-post spiking within a 10 ms timing window gives rise to LTP, whereas post-before-pre firing produces LTD (Bi and Poo, 1998; Debanne et al., 1998; Feldman, 2000; Markram et al., 1997b). Mechanistically, this timing requirement is thought to depend upon nonlinear summation of voltage (Stuart and Häusser, 2001) and calcium signals (Koester and Sakmann, 1998; Magee and Johnston, 1997; Schiller et al., 1998; Yuste and Denk, 1995) produced by EPSPs and back propagating action potentials (AP).

In addition to depending upon the precise temporal structure of coincident firing, induction of plasticity can also depend on the number of coincident inputs. In early studies, this dependence was termed cooperativity: tetanization of a weak pathway produced potentiation only if in synchrony with a stronger pathway (Barrionuevo and Brown, 1983; Debanne et al., 1996; Kirkwood and Bear, 1994; Levy and Steward, 1979; McNaughton et al., 1978; Zalutsky and Nicoll, 1992). More recently, cooperativity has been presumed to reflect the fact that unitary inputs produce small depolarizations (Markram et al., 1997a), which are insufficient to allow enough NMDA-mediated calcium influx to produce LTP (Bliss and Collingridge, 1993). A prediction of this view is that STDP should not exhibit cooperativity, since in these protocols the postsynaptic APs are provided, which should unblock NMDA receptors (Debanne et al., 1996). Here we reexamine this issue and demonstrate a novel form of cooperativity that gates LTP induction depending upon the degree of depolarization immediately preceding the postsynaptic spike.

Rate-dependent and timing-dependent induction of cortical plasticity has served as starting points for influential models of cortical learning and development. Rate-based models typically ignore the details of timing (Bienenstock et al., 1982; Linsker, 1988; von der Malsburg, 1973), while spike timing-based models have typically disregarded the dependence of learning rules on

[1] Correspondence: nelson@brandeis.edu

rate (Gerstner et al., 1996; Song et al., 2000; van Rossum et al., 2000). The integration of these two parameters into a single learning rule is not trivial. For example, at high rates (e.g., 50 Hz) a single postsynaptic AP can occur at a time that is both immediately before one presynaptic AP, and immediately following another. How are the plasticity signals from these multiple timing relationships integrated? Prior modeling studies have assumed either that each postsynaptic spike interacts with all presynaptic spikes equally (Gerstner et al., 1996; Senn et al., 2001; Song et al., 2000) or with the presynaptic spikes immediately preceding and following it (van Rossum et al., 2000). These models make different predictions about the way that plasticity builds up during correlated firing.

Here we have systematically varied the rate, timing and number of coincident afferents in order to explore the rules that govern induction of long-term plasticity between monosynaptically connected thick, tufted L5 neurons in rat visual cortex. Our experiments reveal a joint dependence of plasticity on timing and rate, as well as a novel form of cooperativity operating even when the postsynaptic AP is evoked by current injection. Based on these experiments we have constructed a quantitative description, which accurately predicts the build-up of potentiation and depression during random firing.

Results

We made quadruple whole-cell recordings from thick, tufted L5 neurons in rat visual cortex (Figure 1A). The rate of connectivity was 15% (239 connected pairs of 1604 tested), which is similar to that reported for somatosensory cortex (Markram et al., 1997a). The number of multiply connected cells exceeded that predicted if connection probability were random (e.g., 62/239 pairs were reciprocally connected). This suggests that, as in somatosensory cortex (Markram, 1997), the connectivity of visual cortical L5 neurons is inhomogeneous.

Potentiation in L5 Pairs Is Frequency Dependent

In order to induce LTP, brief current pulses were used to evoke precisely timed pre- and postsynaptic APs 10 ms apart. High frequency bursts of pre-before-post pairing at +10 ms produced LTP (Figure 1B), whereas induction at 0.1 Hz did not give rise to any long-term plasticity (Figure 1C). This frequency relationship (Figure 1D) is similar to that described previously by Markram et al. (1997b) for L5 pairs in rat somatosensory cortex, but differs from that observed for extracellularly evoked inputs to L2/3 pyramidal neurons (Feldman, 2000; see also Bi and Poo, 1998; Debanne et al., 1998; Zhang et al., 1998). Post-before-pre pairing, on the other hand, gave rise to robust LTD at 0.1 and up to 20 Hz (frequency dependence discussed further below). The timing requirements (Figure 1E) were similar to those previously described at other neocortical and hippocampal synapses (Bi and Poo, 1998; Debanne et al., 1998; Feldman, 2000; Gustafsson et al., 1987; Levy and Steward, 1983; Magee and Johnston, 1997; Markram et al., 1997b; Zhang et al., 1998), showing a sharp transition from LTP at +10 ms to LTD at −10 ms. LTD could be evoked over a broader range of timing differences (−10 to at least −50 ms) than LTP (+10, but not ≥ +20 ms).

Both LTP and LTD were sensitive to the NMDA receptor antagonist APV (not shown; Bi and Poo, 1998; Debanne et al., 1998; Feldman, 2000; Magee and Johnston, 1997; Markram et al., 1997a; Zhang et al., 1998). LTP induction at 50 Hz in the presence of APV gave rise to no potentiation (106 ± 3.8%, $n = 4$, $p = 0.89$ as compared to baseline-only experiments). Note that blocking LTP using APV did not give rise to depression as previously reported for L2/3 neurons (Feldman, 2000). LTD induction at 10 or 20 Hz gave rise to no depression in the presence of both APV and the activity dependent NMDA blocker MK-801 (95.8 ± 8.3, $n = 3$, $p = 0.39$).

Potentiation of Extracellularly Evoked Responses at Low Frequency Depends on EPSP Size

As noted above, the absence of pre-before-post potentiation in L5 pairs at 0.1 Hz seemingly conflicts with the observations that L2/3 somatosensory neurons do exhibit pre-before-post LTP at low frequencies using extracellular stimulation (Feldman, 2000). Biological differences, e.g., due to region or synapse type, could account for this disparity. Alternatively, experimental aspects such as presynaptic washout or variations in induction protocol could underlie the discrepancy. In an attempt to resolve the conflicting reports, we set out to reproduce Feldman's protocol in visual cortical L5 neurons using extracellular stimulation. An additional advantage of this approach is that EPSPs of graded amplitude could be obtained with extracellular stimulation. With pre-before-post low frequency induction, extracellularly evoked EPSPs reliably potentiated if the pre-pairing responses were larger than approximately 2mV (Figures 2A and 2C). With extracellular stimulation of smaller amplitude, no LTP was observed (Figures 2B and 2C). This suggested that, at low frequencies, a sufficiently large number of inputs had to be activated in concert to produce LTP in L5 neurons.

One could have surmised that the difference in the number of pairings between the low and high frequency protocols (50 versus 75) could account for the absence of low frequency LTP in pairs. However, this is unlikely, given the frequency dependence of LTP in pairs (Figure 1D) and the robust low frequency LTP for large EPSPs (and for the cooperativity and depolarization experiments described below).

Other properties of extracellular STDP in L5 neurons resembled those reported for L2/3 somatosensory neurons (Feldman, 2000). Post-before-pre pairing gave rise to LTD that developed with a similarly slow time course (Figures 1E and 2C), and that did not seem to depend on the initial EPSP amplitude (Figures 2C and 2D). Furthermore, the spike-timing curve also exhibited an extended timing window for LTD (Figure 2D).

Low-Frequency Potentiation in L5 Pairs Exhibits Cooperativity

If many inputs must act in synergy to produce pre-before-post LTP at low frequencies, it may be possible to rescue potentiation in L5 pairs by coincidence of a sufficiently large extracellularly evoked response with the unitary EPSP during the induction period. Figure 3A illustrates the results of such an experiment, in which

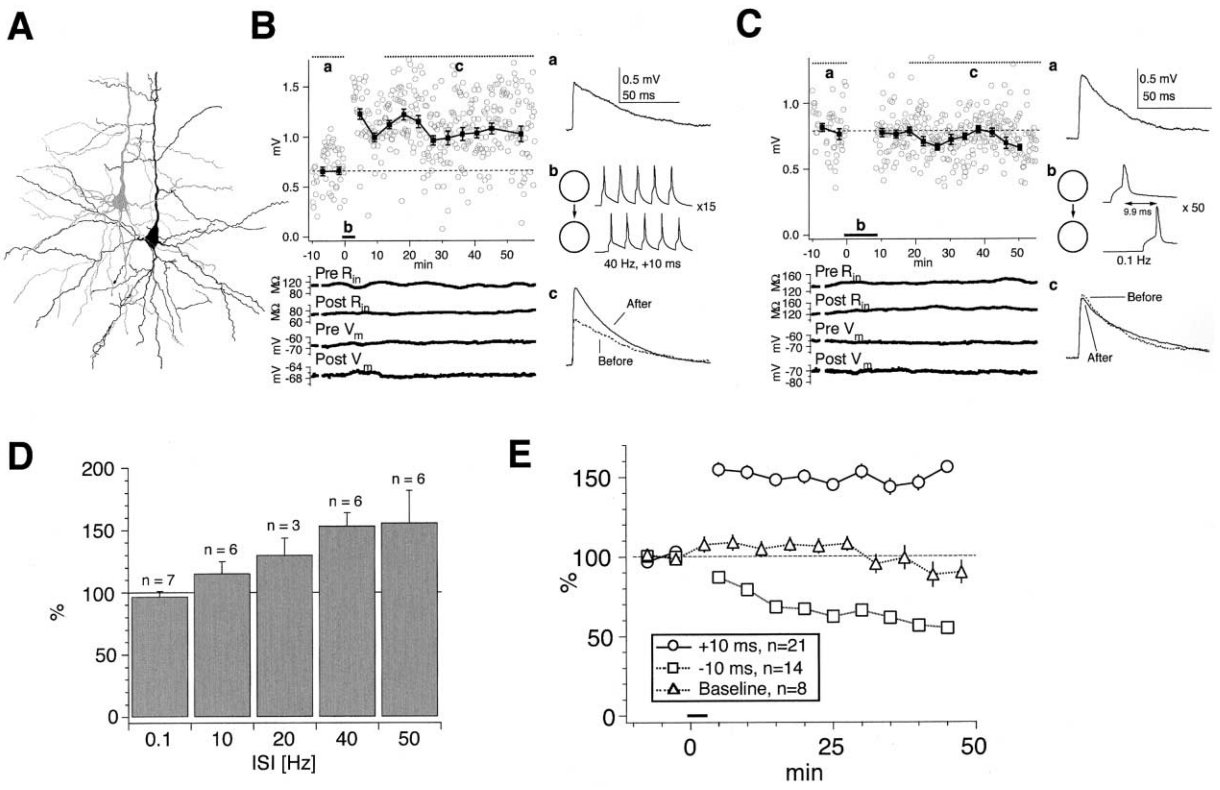

Figure 1. Spike Timing-Dependent LTP in Visual Cortical L5 Pairs Depends on Frequency

(A) Camera lucida drawing of a connected L5 pair. The left cell is presynaptic. Responses are shown in (B).

(B) LTP induction at 40 Hz. Top graph shows individual response amplitudes (open symbols) and five-min averages (filled symbols). Pre- and postsynaptic input resistance and membrane potential (lower traces) remained stable throughout the experiment. Right hand traces illustrate average unitary EPSPs before and after (Ba, Bc) induction (Bb), consisting of 15 bursts of five spikes at 40 Hz with presynaptic spikes preceding postsynaptic spikes by 10 ms (+10 ms). Average EPSP amplitude was potentiated by 163% (after/before, $p < 0.01$).

(C) Failure of LTP induction at low frequency. Responses from another pair in which 50 +10 ms pairings were delivered at 0.1 Hz (Cb) and no potentiation was observed.

(D) Pre-before-post firing (+10 ms) produced LTP at frequencies of 10 Hz and higher. The degree of potentiation increased with frequency.

(E) Pre-before-post firing (+10 ms) at frequencies between 10 and 50 Hz produced LTP (circles, n = 21), while post-before-pre firing (−10 ms) at frequencies between 0.1 and 20 Hz produced LTD (squares, n = 14). Low frequency pairing at large temporal offsets (+ 400 ms) produced little change in EPSP amplitude (triangles, n = 8).

the unitary EPSP was boosted during the induction by a 7.1mV extracellularly generated response, indeed resulting in LTP. Cooperative activation of unitary EPSPs and compound extracellularly evoked EPSPs reliably evoked low frequency potentiation in L5 pairs (Figure 3B). The extracellular responses used for boosting the unitary EPSP also potentiated (data not shown).

A synapse strength histogram was obtained based on a sample of 139 paired recordings (Figure 3C). These data suggested that less than 5% of all L5-to-L5 connections were large enough to permit low frequency LTP on their own. A Monte Carlo simulation based on the fit of a Poisson function (Figure 3C) and a threshold for LTP of 2.3mV (Figure 5A) indicated that, on average, 5.4 ± 1.5 (SD) L5 neurons would have to cooperate to produce LTP.

Low-Frequency Potentiation in L5 Pairs Is Rescued by Depolarization

The source of the cooperativity effect could be a need for a certain amount of postsynaptic depolarization. To test this hypothesis, 100-ms-long depolarizing somatic current injections were delivered during the induction. Figure 4A illustrates an experiment of this type in a reciprocally connected L5 pair, where depolarization did rescue low frequency LTP. Current injection was adjusted so that the postsynaptic cell was depolarized to just below threshold. Precisely timed spikes were then produced with additional brief current steps (Figure 4Ac). This procedure reliably rescued low frequency potentiation, while preserving the spike-timing dependence, so that post-before-pre pairing still gave rise to LTD (Figure 4B). As a control, postsynaptic depolarization with pre- but not postsynaptic firing gave rise to LTD (data not shown, 64.5 ± 6.5%, n = 3, $p < 0.05$). This last result was expected since pairing synaptic activation with subthreshold depolarization had previously been shown to elicit LTD at neocortical synapses (Artola et al., 1990).

The Dependence of LTP and LTD on Depolarization and Frequency

In Figure 5A, all pre-before-post data at low frequency are plotted versus the degree of somatic depolarization

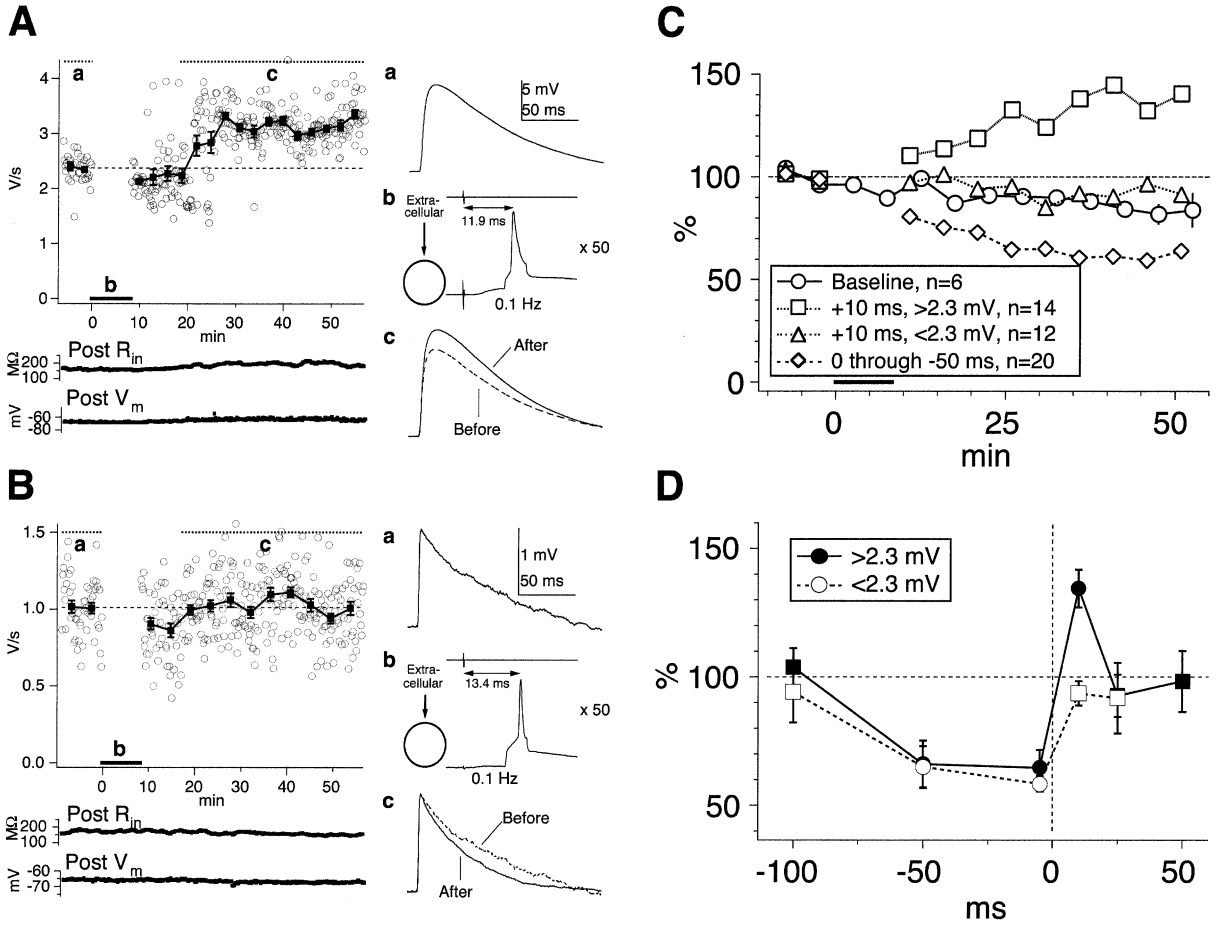

Figure 2. Pre-before-Post Firing Produces LTP at Low Frequency when Using Extracellular Stimulation of Sufficient Amplitude

Plotting conventions are as in Figure 1, except that initial EPSP slope was extracted rather than the peak EPSP amplitude.

(A) For large (>2.3mV) EPSPs low frequency pre-before-post pairing evoked robust LTP. In this example, potentiation of initial slope was 127%, $p < 0.01$.

(B) The same procedure failed to potentiate small EPSPs (<2.3mV). In this example the temporal offset was 13.4 ms, the initial amplitude was 1.4mV, and the potentiation of the initial slope was 102%, $p = 0.47$.

(C) Low frequency pre-before-post pairings produced LTP of large EPSPs (squares, $n = 14$, $p < 0.001$), but not small EPSPs (triangles, $n = 12$, $p = 0.89$). Post-before-pre pairing produced LTD (diamonds, $n = 20$, $p < 0.001$), independently of EPSP size. Low frequency pairing at large temporal offsets (+400 ms) produced little change or slight depression of EPSP initial slope (circles, $n = 6$).

(D) Change in EPSP slope (after/before) is plotted against temporal offset between postsynaptic firing and presynaptic stimulation. Positive offsets are pre-before-post, negative are post-before-pre. The results for large (filled symbols) and small EPSPs (open symbols) were identical, except no LTP was produced for small EPSPs. Circles represent significant ($p < 0.05$) LTP or LTD. The n's are between 3 and 7 per point, except for at +10 ms: 14 for >2.3mV, and 12 for <2.3mV.

(see Experimental Procedures). It is clear that, although the scatter is considerable, there is no potentiation on average below approximately 2mV total depolarization. To quantify the threshold depolarization at which potentiation occurred in visual cortical L5 neurons, a sigmoid was fit, which produced a half-maximum of 2.1mV (Figure 5A). Similarly, a sliding t test for the difference of the means to the left and right of a moving threshold had the highest statistical significance at a threshold value of 2.3mV ($p < 0.001$, Figure 5A, inset). Linear regression gave an R value of 0.41, indicating a correlation between the magnitude of potentiation and amount of depolarization. An important caveat is that we did not systematically explore the threshold voltage for rescue of low frequency LTP by somatic depolarization, but instead used the largest depolarizations that remained subthreshold. It is likely that EPSPs measuring 2.3mV at the soma are significantly larger at the dendrite.

The same type of analysis for LTD suggested no such dependence on the degree of depolarization (Figure 5B). Linear regression produced an R value of 0.097 and $p > 0.05$ at the minimum of the sliding t test (Figure 5B, inset). These data argue that induction of LTP, but not LTD, requires a critical amount of postsynaptic depolarization even in the presence of postsynaptic firing.

It has previously been reported that the amount of LTP is inversely correlated with the initial synaptic strength (Bi and Poo, 1998; Liao et al., 1992; Montgomery et al., 2001). The depolarization threshold for LTP (Figure 5A) appeared to be at variance with this observation. However, plotting the amount of LTP versus the initial synaptic strength, for experiments where potentia-

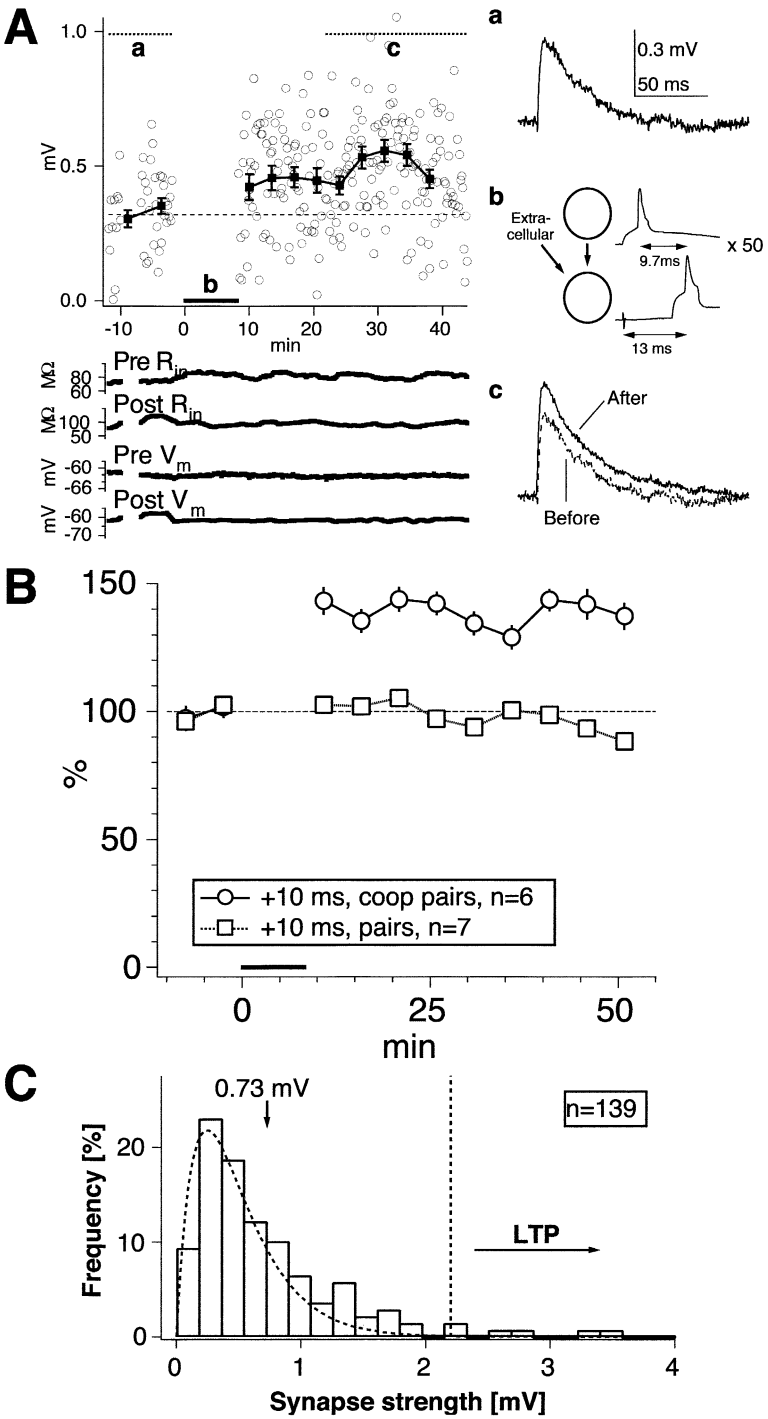

Figure 3. Cooperativity of Low-Frequency Potentiation in Pairs

(A) Extracellular stimulation during induction rescues low frequency potentiation of unitary EPSPs. The extracellularly evoked EPSP (not shown) was 7.1mV. The unitary EPSP amplitude potentiated by 146%, $p < 0.01$.

(B) LTP produced in six pairs by simultaneous unitary and extracellular stimuli delivered ~10 ms before postsynaptic firing at low frequency (circles, 139 ± 4.8%, $n = 6$, $p < 0.01$). The same protocol in the absence of extracellular stimulation produced no significant change in EPSP amplitude (squares, $n = 7$, same data as in 0.1 Hz bar in Figure 1D). For cooperativity experiments, the average extracellularly evoked EPSP amplitude was 6.2 ± 1.8mV, while the average EPSP amplitude from the paired recording was 0.37 ± 0.04mV.

(C) More than 95% of synaptic connections are weaker than the 2.3mV threshold for LTP (vertical dashed line), determined from Figure 5A. The dashed curve is a Poisson function fit.

tion was robust, revealed a weak inverse relationship (Figure 5C). No correlation between the amount of LTD and the initial EPSP amplitude could be found (data not shown).

We noticed that with the high frequency induction protocol, the membrane potential did not quite repolarize to rest between the spikes of the induction spike trains (cf. Figure 5D inset). This was in part due to the spike after-depolarization and in part due to the membrane time constant. The amount of residual depolarization increased with frequency and was of a magnitude sufficient to rescue potentiation (Figure 5D). Furthermore, the amount of LTP obtained at these frequencies correlated well with the amount of residual depolarization (Figure 5E).

To test the hypothesis that the presence of LTP at high frequencies depends upon residual depolarization between spikes, small hyperpolarizing current injections were added between the spikes of the induction spike trains (Figure 6Ab). The example illustrated in Figure 6A

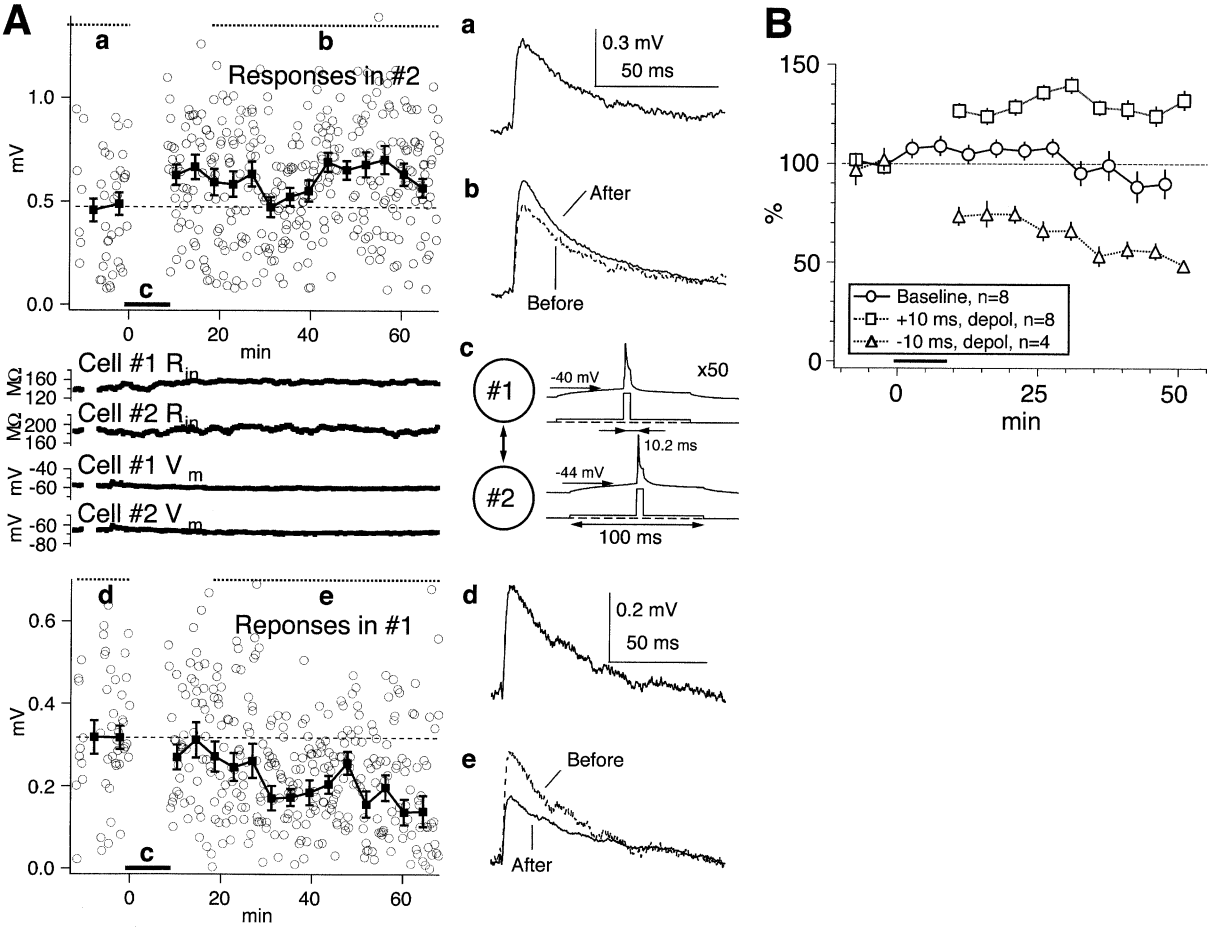

Figure 4. Postsynaptic Depolarization Rescues Low-Frequency Potentiation in Pairs

(A) Depolarization during induction in a bidirectionally connected pair rescues potentiation at +10 ms while preserving depression at −10 ms. Current injection depolarized cells to just below firing threshold during induction. EPSPs in cell 2 potentiated to 130%, $p < 0.01$, (Ab), while EPSPs in cell 1 depressed to 62%, $p < 0.01$ (Ae).

(B) Postsynaptic spikes evoked during depolarization to −45.1 ± 1.7mV reliably rescued potentiation at +10 ms in pairs (squares, 136 ± 9.5%, $n = 8$, $p < 0.05$). Induction at −10 ms during depolarization still brought about LTD (triangles, 64.5 ± 6.5%, $n = 4$, $p < 0.01$). The baseline (circles) is the same as that shown in Figure 1E.

depressed using this protocol, but on average no long-term plasticity was seen (Figure 6B). This pronounced effect ($p < 0.05$ for comparison between 40 Hz induction with and without hyperpolarization) implies that residual depolarization between spikes is required to permit robust pre-before-post LTP in L5 pairs at high frequencies. It should be noted, however, that this cannot entirely explain the frequency dependence of LTP induction since although depolarization was able to rescue induction at low frequency, the amount of LTP was significantly less ($p < 0.05$) than that observed at high frequency (after/before = 136%, 0.1 Hz, Figure 5A, $n = 28$, whereas after/before = 165%, 50 Hz, Figure 5E, $n = 16$).

It has been suggested that in the CA1 region of the hippocampus, transient potassium currents (I_A) may regulate LTP induction by preventing AP back propagation (Hoffman et al., 1997; Migliore et al., 1999). Accordingly, depolarization due to a sufficiently large EPSP may inactivate I_A, thus facilitating AP back propagation, which in turn could enable LTP. To test whether I_A currents were underlying the cooperativity effect, the low frequency protocol illustrated in Figure 6C was employed. The postsynaptic cell was depolarized by subthreshold somatic current injection for 50 ms, then, a short hyperpolarizing current was applied to bring the membrane potential back to rest. At this point, the spike was delivered (cf. Figure 6Cb). With this protocol, at least 60% of I_A currents are still inactivated at the time of the spike, assuming that inactivation recovers with a time constant of at least 15 ms (Bekkers, 2000; Korngreen and Sakmann, 2000). However, no potentiation was evoked using this protocol (Figure 6D), suggesting that I_A inactivation is not the mechanism underlying the cooperativity effect seen in visual cortical L5 neurons. Taken together, these experiments demonstrate that at both low and high frequencies, brief hyperpolarization blocks depolarization-enabled LTP.

We next attempted to ascertain whether depression exhibited a frequency dependence similar to that of potentiation (Figure 1D). No frequency dependence could be measured for LTD at 20 Hz and below, but at 40 Hz and above, depression was nonexistent and instead LTP

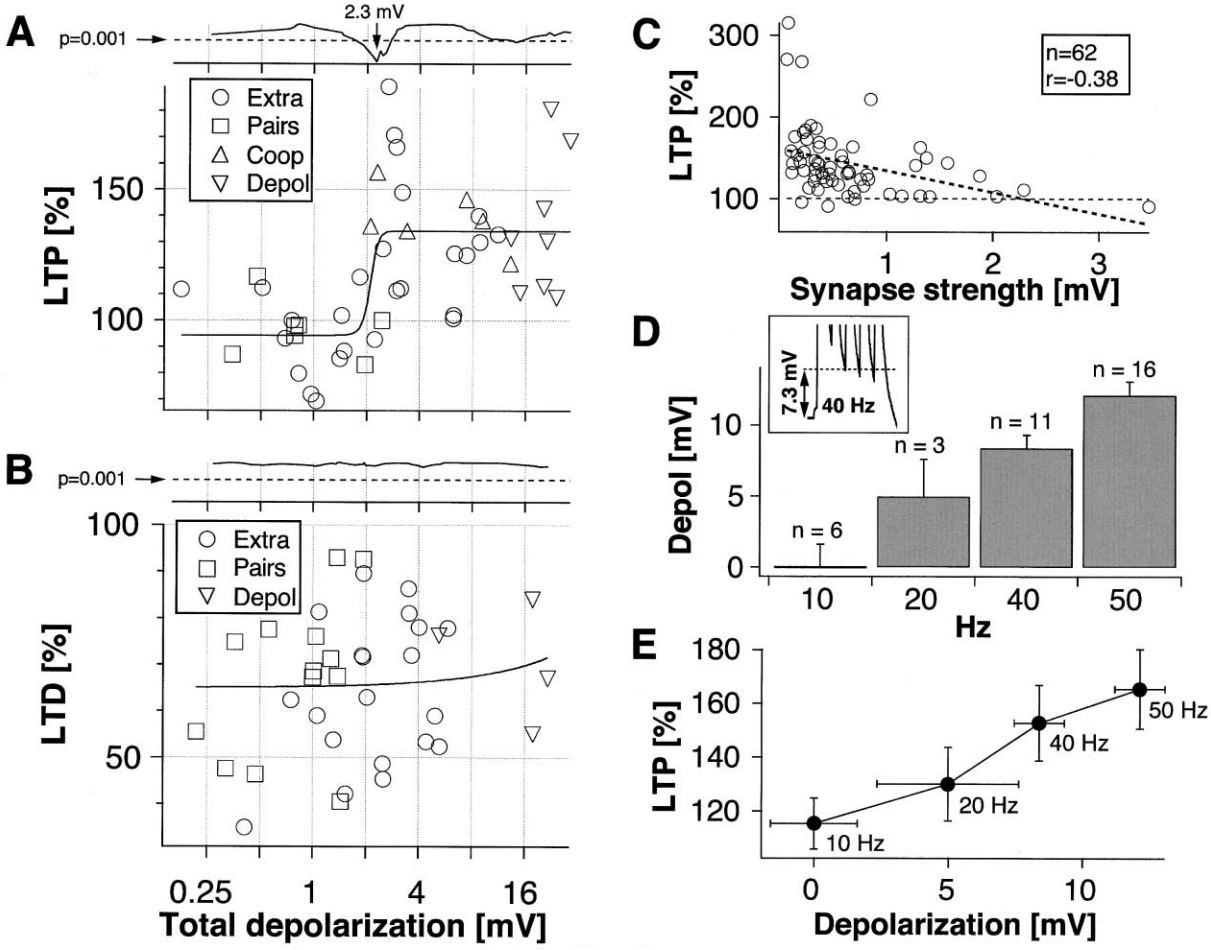

Figure 5. LTP, Not LTD, Depends on Depolarization

(A) All experiments at +10 ms and at 0.1 Hz are shown. Extracellular stimulation experiments are denoted by circles ("Extra"), pairs are signified by squares ("Pairs"), cooperativity experiments (Figure 3) are illustrated by upright triangles ("Coop"), and results obtained with somatic current injection (Figure 4) are shown with upside-down triangles ("Depol"). Approximately 2.3mV depolarization was required for potentation. Best-fit sigmoid had a half-maximum of 2.1mV, while a sliding t test had minimal probability ($p < 10^{-6}$) at 2.3mV (top graph).

(B) Long-term depression does not depend on membrane depolarization. All experiments at 0–50 ms and frequencies 0.1–20 Hz are shown in this plot. Symbols are as in (A). Amount of depression and total depolarization were not correlated ($r = 0.097$). Minimal p as generated by a sliding t test (top graph) was larger than 0.05, suggesting no depolarization threshold for LTD.

(C) The amount of LTP depends inversely on the initial EPSP strength (weak correlation, $r = -0.38$). All data is from paired recordings where robust LTP was obtained: pre-before-post (10–50 Hz, Figure 1D), post-before-pre (40 and 50 Hz, Figure 7B), cooperativity (Figure 3B), depolarization (Figure 4B), random firing (50 Hz, Figure 8C), and synchronous firing experiments (100 Hz, Figure 7D).

(D) Residual depolarization present between spikes depends on frequency. Inset: Membrane potential did not repolarize back to rest between spikes of a 40 Hz burst. In this example, the mean residual depolarization measured 7.3mV.

(E) The degree of potentiation (from Figure 1D) and the amount of residual depolarization (from Figure 5D) at different frequencies are roughly linearly correlated.

was produced (Figure 7B). This finding was most convincingly illustrated in the case of bidirectionally connected L5 pairs, like that shown in Figure 7A. In these cases, the same APs are pre-before-post in one direction, and post-before-pre in the other direction. In each of these cases (n = 4 pairs at 50 Hz and n = 3 pairs at 40 Hz) potentiation was produced in both directions. It should be pointed out that at these frequencies, postsynaptic spikes that fall within the LTD window for one presynaptic spike (e.g., −10 ms in Figure 2D) also fall within the LTP window for the next presynaptic spike (e.g., +15 ms at 40 Hz, or +10 ms at 50 Hz). Hence high frequency trains produce both LTP and LTD timing interactions at the same time. This may explain the absence of LTD at high frequencies (see Discussion).

The complex dependence of long-term plasticity on frequency suggested that accurately predicting plasticity during complex firing patterns might require separately measuring the spike-timing curve at each frequency. Toward that end, we combined the existing data from Figures 1D and 7B (corresponding to the +10 and −10 ms time points) with additional data from experiments designed to fill in the timing curves at 0.1 Hz, 20 Hz, 40/50 Hz and 100 Hz. Data from pairs stimulated at 0.1 Hz (without boosting or depolarization) closely overlapped the more completely studied timing curve

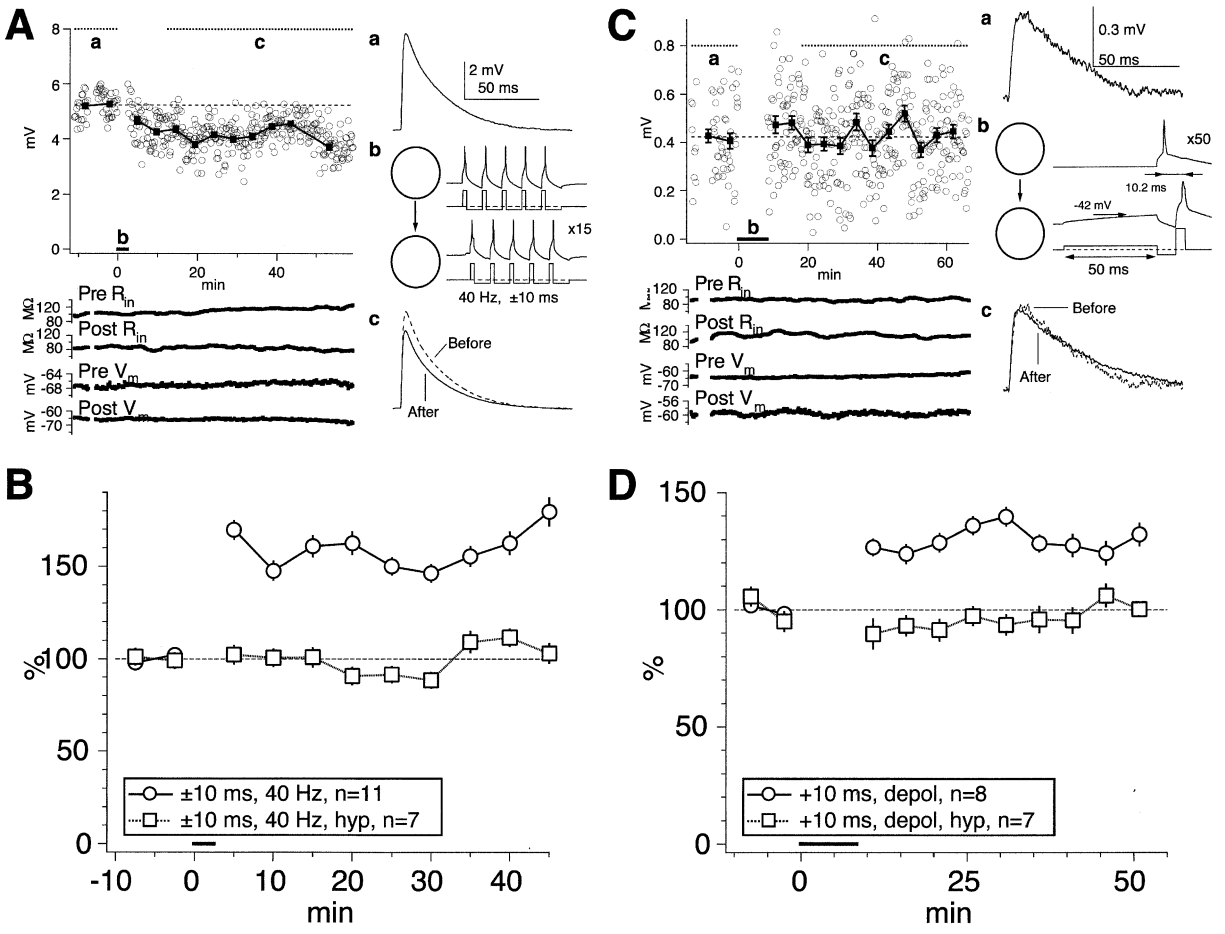

Figure 6. Hyperpolarization Preceding APs Prevents Potentiation

(A) Hyperpolarizing current injection between spikes (Ab) counteracted residual depolarization present at high frequency (cf. Figure 5D), and the membrane potential was brought down approximately to rest. In this example at 40 Hz, the responses depressed to 79% ($p < 0.01$).

(B) Depolarization during 40 Hz firing is required for induction of potentiation. While 40 Hz inductions normally produced a high degree of potentiation (circles, 153 ± 14%, n = 11, $p < 0.05$), modest hyperpolarization to −77.5 ± 1.0mV between the spikes within a burst reliably blocked potentiation (squares, 100 ± 9.1%, n = 7, $p = 0.56$ compared to baseline, $p < 0.05$ compared to normal 40 Hz induction).

(C) Brief hyperpolarization blocks the depolarization-induced rescue of low frequency potentiation. During induction, the postsynaptic cell was depolarized to just below firing threshold for 50 ms. The cell was then quickly repolarized back to roughly the membrane potential before the spike was delivered. In this example, the time between the end of the depolarization and the spike was 14 ms (Cb). Responses remained unchanged in this pair: 99.2%, $p = 0.89$ (Cc).

(D) At +10 ms, uninterrupted depolarization rescued low frequency potentiation (circles, reproduced from Figure 4B for comparison), while depolarization interrupted by hyperpolarization did not (squares, 95.8 ± 6.7%, n = 7, $p = 0.27$ compared to baseline, $p < 0.01$ compared to uninterrupted depolarization). Duration of interruption was 7.3 ± 1.8 ms.

derived from small amplitude extracellular stimulation (Figures 7C and 2D). As expected from the lack of voltage dependence of LTD, these curves differ from those obtained with large amplitude extracellular stimuli only in that they lack an LTP portion (cf. Figure 2D). At 20 Hz, synchronous firing ($\Delta t = 0$ ms) produced somewhat more LTD than at 0.1 Hz, and LTD was also evident when $\Delta t = +25$ ms. Both of these effects can be understood in terms of multiple spike-timing interactions and the low frequency spike-timing curve. At 20 Hz, a postsynaptic spike at $\Delta t = 0$ ms falls within the LTD window of the subsequent presynaptic spike ($\Delta t = -50$ ms). Similarly, a Δt of +25 ms is equivalent to a Δt of −25 ms for the subsequent presynaptic spike. At 40 and 50 Hz, the entire interaction window is only ± 12.5 or 10 ms, respectively; timings outside this range are equivalent with respect to a subsequent or preceding spike. As noted above, LTD at $\Delta t = -10$ ms disappears at these frequencies, presumably because additional timings that produce LTP are also present; each postsynaptic spike with $\Delta t = -10$ ms, also has a $\Delta t = +10$ ms (50 Hz) or +15 ms (40 Hz) with respect to the preceding presynaptic spike. It is important to note, however, that the disappearance of LTD does not mean that plasticity was no longer timing dependent. This can be observed from the fact that synchronous firing ($\Delta t = 0$ ms) produced no LTP at 40 Hz (Figures 7C and 7D). As frequency continues to rise, postsynaptic spikes, which are precisely synchronized with presynaptic spikes, begin to approach the LTP window for the preceding presynaptic spike. This effect is marked at 100 Hz, in which case robust LTP is induced (Figure 7D). Here, each postsyn-

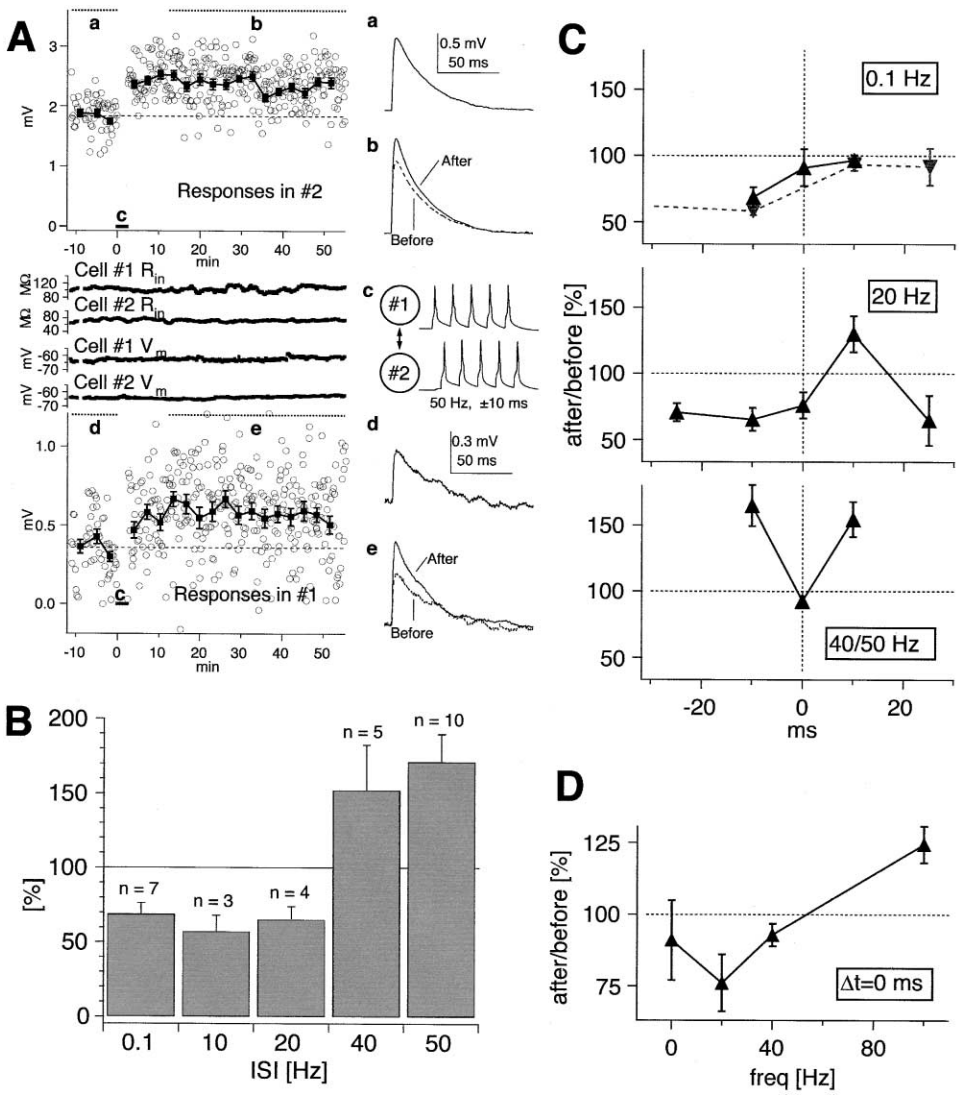

Figure 7. At and above 40 Hz, LTD Is Absent

(A) In a bidirectionally-connected pair, induction at 50 Hz gave rise to potentiation in both directions. Note that although the first spike in cell 2 is 10 ms after the first spike in cell 1, it is also 10 ms before the second spike in cell 1. The EPSPs recorded in cell 1 potentiated to 163%, $p < 0.01$, while those recorded in cell 2 potentiated to 128%, $p < 0.01$.

(B) Depression did not show any frequency dependence at low frequencies, but did not exist at and above 40 Hz.

(C) Spike-timing curves obtained at 0.1, 20, and 40/50 Hz in paired recordings indicated that depression predominated at low frequency, whereas potentiation was more prevalent at high frequencies. The n's are between 3 and 7 per point, except for +10 ms and −10 ms at 40/50 Hz (n = 12 and 15, respectively). Dashed trace at 0.1 Hz show extracellular stimulation experiments for EPSPs < 2.3mV for comparison (taken from Figure 2D).

(D) Synchronous firing at frequencies up to 40 Hz resulted in depression, whereas potentiation was obtained at 100 Hz. The n's are between 3 and 5 per point.

aptic spike has a $\Delta t = +10$ ms with respect to the preceding presynaptic spike, $\Delta t = 0$ ms with the current presynaptic spike, $\Delta t = -10$ ms with the subsequent postsynaptic spike. The frequency at which the net effect of these multiple pairings shifts from LTD to LTP is determined by the width of the LTP window (~20 ms corresponding to ~50 Hz).

The dramatic changes in the shape of the spike-timing curve with frequency (Figure 7C) underscore the importance of jointly considering timing and frequency in the induction of plasticity. However, the fact that the shape changes can be largely understood in terms of multiple spike interactions raised the possibility that data at all frequencies could be explained using a single set of time windows for induction of LTP and LTD. This idea is explored quantitatively in the next section.

Modeling the Dependence of Plasticity on Timing, Rate, and Depolarization

The consequences of LTP and LTD for cortical learning and development have previously been investigated using neural simulations. The build-up of plasticity during irregular correlated firing depends critically on how multiple spike interactions are integrated. Most previous

models have assumed that all spike interactions falling within the range of delays given by the spike-timing curve (e.g., +20 to −75 ms) contribute equally (Gerstner et al., 1996; Senn et al., 2001; Song et al., 2000). Alternatively, only the nearest neighbor interactions may contribute. A local interaction rule of this sort has been used by van Rossum et al. (2000). Implicit in both approaches is the assumption that a single spike-timing curve governs interactions at all frequencies. To test this assumption and quantify the rules that govern long-term plasticity at L5 synapses, three phenomenological computer models were formulated. All three models involved the following steps: First, the polarity of the predicted plasticity contributed by each pair of correlated pre- and postsynaptic spikes were determined from the time interval between them. Spike pairs with $+20 > \Delta t > 0$ ms generated LTP, spike pairs with $0 > \Delta t > -75$ ms generated LTD, and spike pairs outside of this window were ignored. Next, for spike pairs within the LTP window, the magnitude of LTP was determined jointly by the membrane potential immediately preceding the postsynaptic spike and by the instantaneous frequency. The voltage dependence was determined from the sigmoidal fit to the data in Figure 5A. The residual depolarization is itself frequency dependent (Figure 5E). However, as mentioned above, the fact that maximal LTP at high frequency exceeds maximal LTP at low frequency implies a second component of frequency dependence. This was modeled linearly. Hence for all three models, the only parameters varied in the fitting process were the slope and intercept of the frequency dependence. These parameters were derived from weighted fits to the frequency dependence of pre-before-post (Figure 1D) and post-before-pre firing (Figure 7B). Finally, the three models differed in which pre- and postsynaptic spikes were permitted to interact:

- Model 1 counted all spike interactions, e.g., several spikes falling in the LTD or LTP windows would sum linearly.
- Model 2 counted only nearest-spike interactions.
- Model 3 was identical to Model 2, except spike interactions producing LTP were presumed to "win" over those producing LTD. This rule was motivated by the results presented in Figures 7B and 7C. It was implemented by not counting LTD interactions whose postsynaptic spike participated in an LTP interaction.

As illustrated in Figure 8A, Models 2 and 3 captured the data significantly better than Model 1; the root-mean-squared error (RMS) was considerably lower for the former models than for the latter. Models 2 and 3 performed nearly equally well. The ability to closely fit the data using a single set of LTP and LTD timing windows validates this approach and argues that it is not necessary to derive the full spike timing curve at all frequencies.

In order to test the generality of the models, each was used to predict the build-up of plasticity in an additional set of experiments in which the precise timing of individual APs was varied randomly. As in the constant frequency experiments, the number of bursts, the number of spikes within a burst, and the mean firing rate within a burst were kept constant. The example shown in Figure 8B was done at a mean rate of 50 Hz. Random firing (Figure 8Bc) produced LTP (Figure 8Ba), even though post-before-pre and pre-before-post timings occurred equally often (Figure 8Bb). The same procedure was repeated at rates of 0.1, 20, and 35 Hz, always with an average timing difference of 0 ms. LTP was robustly produced at high frequency, whereas low frequency random firing gave rise to robust depression (Figure 8C) (Feldman, 2000). Imprecisely timed spiking during the induction thus isolates the rate-based component of plasticity.

Next, we used the model fits to predict the amount of LTP or LTD obtained with random firing at different frequencies (Figure 8C). The RMS was considerably better for Model 3 as compared to both Models 1 and 2 (Figure 8D). Furthermore, linear regression analysis for predicted versus actual magnitude of LTP/LTD gave both better correlation and a slope closer to one for Model 3 ($r = 0.98$, slope $= 1.09$) than for Model 1 ($r = 0.83$, slope $= 0.53$) and Model 2 ($r = 0.92$, slope $= 0.77$).

We conclude from these modeling studies that LTP and LTD interactions occurring closely in time do not sum linearly, but that LTP wins over LTD. Furthermore, multiple interactions (in either the LTP or the LTD window) do not count more than single interactions. The simple rules implemented in Model 3 may provide a more quantitative framework for understanding the impact of correlated firing on synaptic strength.

Discussion

Results presented here describe systematically how long-term plasticity at synapses between thick, tufted L5 neurons depends jointly on firing rate, spike timing and cooperativity among inputs. Previous studies have focused either on the rate or on the timing of pre- and postsynaptic firing, which has lead to an artificial dichotomy between STDP and classical LTP/LTD. At any given rate, the precise timing of pre- and postsynaptic firing is a crucial determinant of the sign and magnitude of plasticity (Figures 2D and 7C). Conversely, for any particular timing, or for random firing, there is a strong dependence of plasticity on rate (Figures 7D and 8C). The measured dependence on rate and timing can be combined into a quantitative description, which accurately predicts the frequency dependence of LTP and LTD evoked by random firing. Such a description is necessary for extrapolating from the simple protocols used in cellular plasticity experiments to the complex firing patterns of neurons in the developing cortex in vivo. Moreover, we find a novel form of cooperativity that is a prominent feature of STDP at low frequencies.

Cooperativity Requirement

Studies of hippocampal synapses have demonstrated that cooperation of many presynaptic fibers is often needed to produce LTP (Debanne et al., 1996; Levy and Steward, 1979; McNaughton et al., 1978; Zalutsky and Nicoll, 1992). This cooperativity presumably reflects the fact that, as in neocortex, individual unitary synapses are too weak to cause strong postsynaptic activation. Consistent with this, the cooperativity requirement is not present when using a classical pairing protocol with

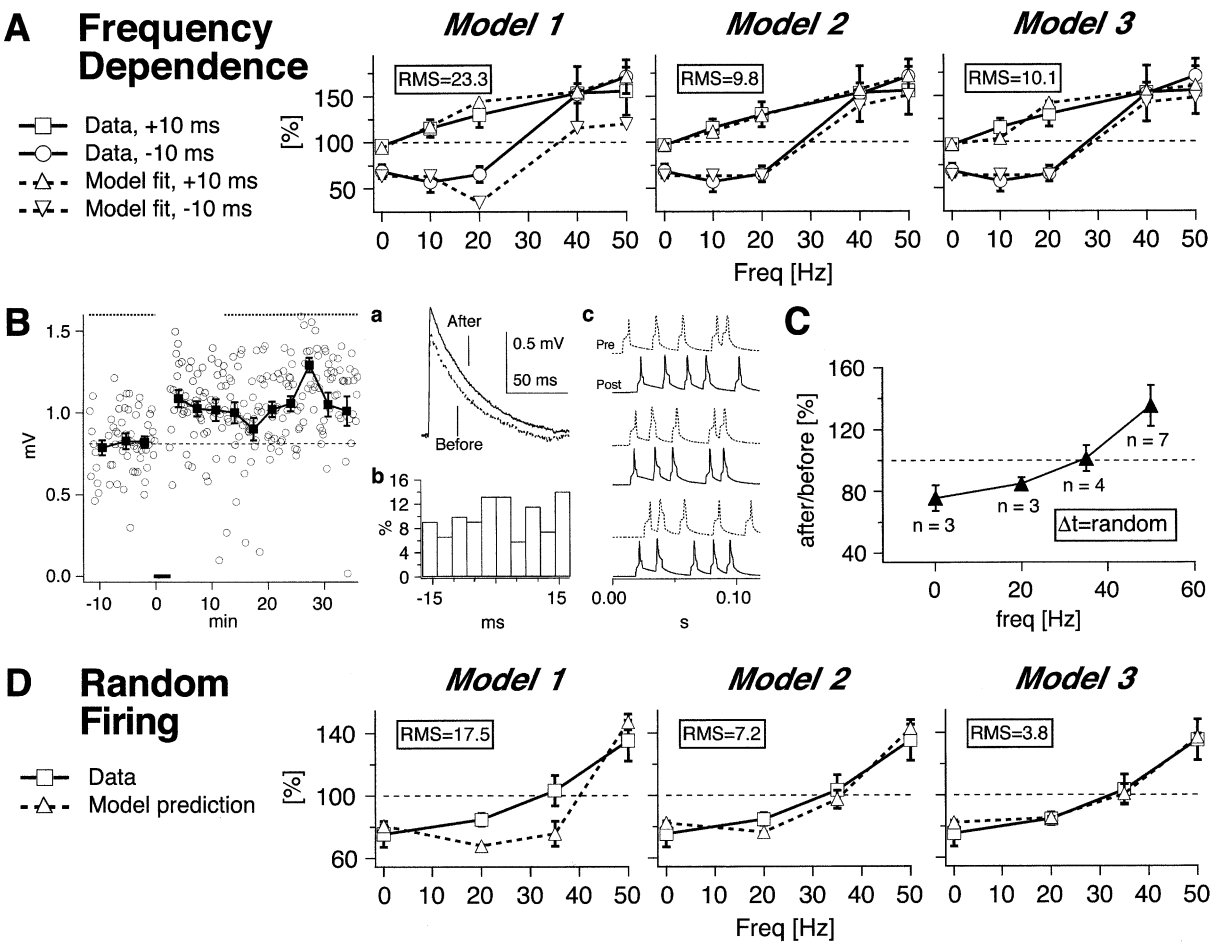

Figure 8. A Quantitative Model Predicts the Effect of Random Firing on Synaptic Plasticity

(A) Models 2 and 3 fit LTP/LTD frequency dependence data best. RMS denotes root-mean-squared error.

(B) Random firing at 50 Hz produced potentiation. The random spiking (3 of 15 induction traces illustrated in Bc) was equally distributed as pre-before-post and post-before-pre interactions (Bb), yet LTP was produced (Ba).

(C) Random firing isolated the rate-sensitive component of long-term plasticity.

(D) Model 3 captured the random firing data best, corroborating the idea that LTP interactions may annul LTD pairings on a short timescale.

postsynaptic depolarization to 0mV (Malinow, 1991). Here we demonstrate a novel form of cooperativity that is present even when the postsynaptic AP is evoked by current injection. We confirmed prior reports that low frequency pairing of unitary inputs and a single postsynaptic spike are ineffective in producing LTP (Markram et al., 1997b), but show that these unitary inputs can be effective when the postsynaptic spike is preceded by modest depolarization. This depolarization can be provided either by concurrent synaptic input (Figure 3) or by somatic current injection (Figure 4).

What mechanism might underlie this form of cooperativity? One explanation is that voltage-gated channels produce a supralinear effect locally at the synaptic sites (Schiller et al., 2000; Wei et al., 2001). In a contrasting view, Stuart and Häusser (2001) have recently shown that back propagating APs in L5 neurons are amplified and propagated more securely in the presence of modest dendritic depolarization. This effect has also been shown to occur in biophysical simulations of CA1 neurons (Migliore et al., 1999). In both cases, the effect is pronounced for distal regions of the apical dendrite (>400 μm from the soma). Synapses between thick, tufted L5 neurons are primarily located on the basal dendrites (Markram et al., 1997a). Recent simulations suggest, however, that the attenuation of back propagating APs, which happens more distally for inputs onto the apical dendrite, may happen much more proximally on the finer, more highly branched, basal dendrites (Vetter et al., 2001).

Depolarization could enhance back propagation either by enhancing sodium channel activation (Stuart and Häusser, 2001), or by inactivating transient potassium current such as I_A (Hoffman et al., 1997; Migliore et al., 1999). Our data suggest that of the two mechanisms, I_A inactivation is less likely. Brief hyperpolarizations (3–10 ms) were sufficient to completely erase the effects of the preceding depolarization. Recently published studies of I_A currents in L5 neurons (Bekkers, 2000; Korngreen and Sakmann, 2000) indicate that these channels should still be largely inactivated at the time of the postsynaptic spike. If I_A inactivation were required for LTP induction,

uninterrupted depolarization (Figure 4) and briefly interrupted depolarization (Figures 6C and 6D) should be nearly equally effective at rescuing LTP induction at low frequency. Instead, we found that at low frequencies interrupted depolarization did not produce any LTP (Figures 6C and 6D), arguing against an involvement of I_A. Furthermore, it was reported that—as opposed to CA1 pyramidal neurons (Hoffman et al., 1997)—thick, tufted L5 neocortical neurons express relatively low levels of I_A along the apical dendrite (Bekkers, 2000; Korngreen and Sakmann, 2000) and that dendritic I_A currents are not inactivated by EPSPs of sufficient amplitude to amplify APs (Stuart and Häusser, 2001).

Cortical neurons recorded in vivo can have somewhat more depolarized membrane potentials (-62 ± 9mV, Moore and Nelson, 1998) than in slice (-64.7 ± 0.3mV, present study). If this reflects a net excitatory effect of increased spontaneous synaptic input, rather than, for example, damage associated with more difficult recording conditions, the need for cooperativity in vivo may be diminished. On the other hand, imaging of cortical dendrites in vivo reveals strong attenuation of somatic APs (Svoboda et al., 1999). In addition to causing depolarization, higher rates of spontaneous activity can reduce input resistance (Paré et al., 1998), which may in turn restrict propagation (Tsubokawa and Ross, 1996) and hence increase cooperativity requirements. Resolving the question of which of these effects predominate will require measuring the dependence of LTP induction on depolarization and EPSP size in vivo.

Dependence on Frequency

Classical LTP and LTD depend on tetanization frequency, so that LTD is evoked at low frequencies, whereas LTP is produced at high frequencies (Dudek and Bear, 1992; Kirkwood et al., 1993; Mulkey and Malenka, 1992). Mechanistically, this is presumed to reflect the ability of a tetanus to evoke postsynaptic firing and a much larger and more rapid rise in postsynaptic calcium (Lisman, 1989; Yang et al., 1999). In contrast, several studies have reported robust induction of LTP when EPSPs are paired with postsynaptic spikes at low frequency, although these studies involved much larger EPSPs due to the fact that they were evoked extracellularly (Feldman, 2000; Zhang et al., 1998) or in culture where unitary inputs are larger (Bi and Poo, 1998; Debanne et al., 1998). The present results strongly suggest that the failure to observe low frequency STDP-induced LTP (Markram et al., 1997b) results from the small size of unitary EPSPs in slice and the need for postsynaptic firing to be preceded by a threshold level of dendritic depolarization. Consistent with this idea, during high frequency bursts, the membrane potential failed to fully repolarize between APs and this residual depolarization permitted robust LTP induction. A greater effectiveness of postsynaptic bursting for inducing plasticity has also been reported in CA1 pyramidal neurons (Pike et al., 1999), although it is unclear in this case whether or not the effect is due to residual depolarization or to some other effect of the burst. Similar results have been obtained in CA3 slice culture, where postsynaptic bursts rescue potentiation of unitary EPSPs (Debanne et al., 1996).

The causal relationship between residual depolarization and LTP induction in our experiments was supported both by their strong correlation (Figure 5E), and by the fact that brief hyperpolarizations between successive APs in a postsynaptic burst blocked induction of LTP (Figures 6A and 6B). These latter results are also in general agreement with several reports showing that inhibition may block LTP (Artola and Singer, 1987; Douglas et al., 1982; Kirkwood and Bear, 1994) and reduce AP back propagation (Tsubokawa and Ross, 1996).

The depolarization requirement for LTP cannot entirely account for the observed frequency dependence. STDP induction at 0.1 Hz in the presence of sufficient depolarization gave rise to significantly less LTP than induction at 50 Hz, and pairing unitary EPSPs with postsynaptic depolarization to 0mV produces potentiation on the order of several hundred percent (Sjöström and Nelson, our unpublished data). This suggests that there may be an integrator at some downstream signaling cascade, which is sensitive to pairing frequency or to the rate and magnitude of calcium influx.

Frequency and Voltage Requirements for LTD

Unlike spike-timing LTP, we found that STDP-based LTD could readily be induced at low frequencies in the absence of preceding postsynaptic depolarization. Also in contrast to LTP, LTD was entirely absent at high frequencies. Both observations are consistent with the proposal that large brief elevations of intracellular Ca^{2+} give rise to LTP, while smaller, slower elevations of Ca^{2+} produce LTD (Lisman, 1989; Yang et al., 1999). At low frequency, pre-before-post spiking causes supralinear summation of voltage (Stuart and Häusser, 2001) and calcium signals (Koester and Sakmann, 1998; Magee and Johnston, 1997; Schiller et al., 1998; Yuste and Denk, 1995). However, at sufficiently high frequencies post-before-pre spiking also causes back propagating APs and EPSPs to coincide, since each presynaptic spike (except the last one) occurs not only immediately after a postsynaptic spike, but also immediately prior to the next postsynaptic spike. Supralinear summation should therefore bring local calcium above the regime associated with LTD, into the regime associated with LTP. Therefore, the disappearance of LTD at 40 and 50 Hz is consistent with a learning rule in which relative pre- and postsynaptic timings giving rise to LTD (-10 ms) are ignored in the presence of relative timings giving rise to LTP.

Computer Modeling Studies

Our modeling studies suggest that cortical plasticity at L5 synapses is best captured by a model where LTP/LTD is jointly determined by firing rate, depolarization, and spike timing, and where only nearest neighbor timing interactions matter. The models did not include reduced LTP of strong inputs (Bi and Poo, 1998; Liao et al., 1992; Montgomery et al., 2001; van Rossum et al., 2000) since the occurrence of strong, paired connections was rare (Figure 3C) and since the inverse correlation between LTP and synaptic strength was relatively weak (Figure 5C).

How can the nearest neighbor rule be understood? In the case of LTP, it could be explained if supralinear summation saturates so that coincidence of a back

propagating AP with two closely overlapping EPSPs produces the same calcium influx as coincidence of the AP with one EPSP. Similarly, saturation may explain the nearest neighbor rule for LTD. This could occur in one of two ways. The rate at which LTD-generating signals build up could saturate at low rates, so that, for example, a single EPSP occurring after a postsynaptic spike produces as much of this signal as two EPSPs within the same LTD window, or as a single EPSP proceeded by two postsynaptic spikes. Alternatively, the total amount of LTD expressed at a given set of synapses could saturate after a modest number of pairings. Further quantitative studies of the dependence of LTD on the number of pairings would be needed to address such issues.

Functional Consequences

The absence of LTD at high frequency underscores another dimension of the often-noted instability of Hebbian plasticity (Miller, 1996; Turrigiano, 1999; Turrigiano and Nelson, 2000). This finding suggests that other mechanisms must contribute to maintaining stability in the face of plasticity. It is likely that multiple homeostatic mechanisms contribute, including enhanced inhibition (Christie et al., 2000; Perez et al., 2001), reduced LTP of strong inputs (Figure 5C) (Bi and Poo, 1998; Liao et al., 1992; Montgomery et al., 2001; van Rossum et al., 2000), enhanced short-term synaptic depression (Finnerty et al., 1999; Markram and Tsodyks, 1996), and synaptic scaling (Turrigiano et al., 1998; Turrigiano and Nelson, 2000; Watt et al., 2000).

There is tremendous ongoing debate as to whether information in cortical circuits is carried primarily by the average firing rate or by the precise timing of correlated APs (see Gray, 1999; König et al., 1996; Shadlen and Movshon, 1999 for reviews). The present results demonstrate that both signals are important determinants of synaptic strength. Interestingly, precisely synchronous firing in the γ frequency range ($\sim$40 Hz), which has been suggested to play an important role in binding disparate elements of cortical circuits, is not itself likely to produce strengthening of the synapses between coactive neurons. Precisely synchronous activity becomes a potent stimulus for inducing LTP only at somewhat higher firing frequencies. Nevertheless, such oscillatory activity patterns could play a role in selectively strengthening synapses active immediately preceding the synchronous events, while weakening subsequently active synapses. The quantitative description developed here may permit future modeling studies to address these and related hypotheses in a more detailed and realistic way. Ultimately, however, tests of these hypotheses will require measurement and manipulation of cortical plasticity during the relevant brain states in vivo.

Experimental Procedures

Electrophysiology

Three hundred micron-thick, slices were cut from visual cortex of Long-Evans rats age P12–P21. Rats were anesthetized with isoflurane, decapitated, and the brain was rapidly removed to ice cold artificial cerebrospinal fluid (ACSF, in mM: NaCl, 126, KCl, 3; $MgCl_2$, 1; NaH_2PO4, 1; $CaCl_2$, 2.5; $NaHCO_3$, 25; Dextrose, 25; osmolality 320 mOsm, bubbled with 95% O_2/5% CO_2, pH 7.4). Slices were cut on a Series 1000 Vibratome (Technical Products International Inc., O'Fallon, MI), moved to ACSF at 36°C, and allowed to cool to room temperature after 10 min. Slices were used after at least one hr of incubation, and up to nine hr after slicing. Recordings were done at 32–34°C. Racemic APV was used at 100 μM concentration. MK-801 (1 μM) was used in addition to APV in some experiments, in order to more fully block NMDA receptors.

Current clamp recordings were obtained using AxoPatch 200B, AxoPatch-1B, and AxoClamp 2B amplifiers (Axon Instruments Inc., Foster City, California) using custom software running on Igor Pro (WaveMetrics Inc., Lake Oswego, Oregon). Data were filtered at 5 kHz and acquired using MIO-16E boards (National Instruments, Austin, Texas) on PowerMacintosh computers (Apple Computer, Cupertino, California). Series resistance (typically 15 MΩ) was not compensated.

Whole-cell recording pipettes (5–10 MΩ, 1–2 μm diameter) were pulled on a P-97 Flaming-Brown Micropipette Puller (Sutter Instruments Co., Novato, California) and filled with (in mM): KCl, 20; (K)Gluconate, 100; (K)HEPES, 10; (Mg)ATP, 4; (Na)GTP, 0.3; (Na)Phosphocreatine, 10; and 0.1% w/v Biocytin, adjusted with KOH to pH 7.4, and with sucrose to 290–300 mOsm.

Extracellular stimulating electrodes (tip diameters of 5–50 μm) were filled with ACSF and placed in lower layer four, 10–50 μm from the apical dendrites of recorded L5 cells. Inhibition was not blocked. Contamination of extracellularly evoked EPSPs by inhibition was revealed by depolarization to just below spiking threshold. Recordings showing any inhibitory contamination were discarded.

Thick tufted L5 neurons were identified at 400$\times$ magnification using infrared DIC optics (Olympus BX-50, Olympus, Melville, New York). Slices were used only if the apical dendrites of superficial L5 neurons were intact and could be traced all or most of the way up to the pial surface. The identity of the neurons was verified after the experiments by biocytin histochemistry (Vectastain ABC Elite kit, Vector Labs, Burlingame, California).

Experiments were discarded or terminated if membrane potential changed more than 8mV or input resistance (measured from 250-ms-long 25 pA hyperpolarizing pulses preceding each trace) changed more than 30%. With these criteria, spike amplitudes and widths remained constant to within 20%, and, as estimated from a sample of 34 experiments, the membrane potential changed less than 1mV on average during the baseline period, and less than 0.8mV during the induction. The same sample revealed no correlation between any trends in the membrane potential and the amount of LTP obtained. Input resistance traces shown in figures were smoothed using box smoothing (15 point window). Series resistance was checked by fitting a double exponential to the initial portion of the hyperpolarizing current step, but was typically not calculated continuously.

The membrane potential of a sample of 271 L5 neurons averaged -64.7 ± 0.30mV (not corrected for junction potential) and did not vary significantly over the range of ages used. The input resistance was 173 ± 6.4 MΩ. This property varied somewhat with the age, e.g., 191 ± 12 MΩ at P14 and 142 ± 16 MΩ at P21 ($p < 0.01$).

Long-Term Plasticity Induction Protocols

Giga-ohm seals were obtained on four neurons, after which whole-cell recordings were established in quick succession to prevent unequal LTP washout. Averaging ten traces assessed connectivity. Hence, potential connections of very low release probability were not used in these experiments.

In all experiments, all involved neurons were made to spike every 10 s throughout the entire experiment. Spikes were produced by 5-ms-long current injections (0.8–1.5 nA). Spikes displaced by at least 400 ms relative to each other, to avoid accidental STDP induction, established baseline.

For experiments using extracellular stimulation and with pairs at low frequency (0.1 Hz), spike delays were shifted during the induction period (50 pairings) to produce the desired spike timing, without changing the overall rate of firing (Feldman, 2000). Induction protocols at high frequency (10 Hz and higher) were done as described by Markram et al. (1997b). Spike trains consisting of five spikes at the desired frequency were paired 15 times at 0.1 Hz, thus producing 75 spike pairings in total. The number of pairings was different for the low and the high frequency protocols in order to keep the results

comparable to the previous literature (Feldman, 2000; Markram et al., 1997b).

For the random firing experiments, timing differences between individual pre- and postsynaptic spikes were drawn from a Gaussian distribution with a SD of 7 ms and 0 mean. High-frequency random firing was in bursts of five spikes repeated every 10 s. Low frequency random firing was at 0.14 Hz. The total number of pairings was 75 at all frequencies.

After the induction period, responses were monitored as before for as long as possible or up to a total recording time of 80 min.

The degree of potentiation or depression was measured as the average response starting 10 min after the induction period until the end of the recording divided by the average response obtained during the initial baseline period. Failures were included in these measurements. A small number of aberrant responses due to electrical artifacts or to spontaneous activity were occasionally removed from these measurements. Recordings were typically 60 min long and were not included if shorter than 40 min.

Analysis and Statistics

Total depolarization (Figures 5A and 5B) was calculated as follows: for pairs and extracellular stimulation experiments it was simply the averaged baseline EPSP amplitude. For cooperativity experiments (Figure 3), the average amplitude of the extracellularly evoked EPSP was added to that of the pair. For depolarization experiments (Figure 4), the average difference in voltage measured 1 ms before the spike and 1 ms before the somatic current injection was added to the EPSP.

The amount of depolarization illustrated in Figures 5D and 5E was extracted in a similar manner. The membrane potential was measured in a 1 ms time window just before the spikes of a spike train (excepting the first spike), averaged, and the membrane potential before the spike train was subtracted from this value.

Synapse strength (Figures 3C and 5C) was based on the average of the approximately 60 responses obtained during the 10 min baseline period.

Comparisons were made by unpaired Student's t test for equal means. Statistically significant change in individual experiments was measured by testing for the change in the average response in the postpairing period as compared to the baseline. Statistically significant change for a particular condition was tested by comparing the averaged percent change after/before induction versus experiments without induction. Means are reported as $\pm$ SEM unless otherwise specified.

For the sliding t test (insets in Figures 5A and 5B), the threshold (d_t) was varied between 0.25 and 20mV and a t test was performed for data points above and below d_t. A clear minimum in p, which was highly significant ($p < 0.001$), suggested the existence of a threshold at the corresponding value of d_t (inset Figure 5A). This method was preferred over the sigmoidal fit (Figure 5A), because the numerically fitted sigmoid was sensitive to initial conditions and would occasionally not converge.

Computer Modeling

The total amount of LTP and LTD was calculated separately and summed. The contribution of one LTD interaction was derived from the mean amount of LTD obtained in Figure 7B at 0.1, 10, and 20 Hz divided by the total number of pairings. The contribution of each LTP pairing depended sigmoidally on the residual depolarization (parameters taken from fit in Figure 5A) and linearly on the instantaneous frequency. The depolarization was measured in a 1 ms-wide window just before the postsynaptic spike, and the instantaneous frequency was taken between that same spike and the one preceding it.

The LTP window was assumed to be $+20 > \Delta t > 0$ ms, since no LTP was produced at $\Delta t = +25$ ms (Figure 2D), whereas LTP was obtained at $\Delta t = +15$, $+10$, and $+5$ ms (Figure 2D; data not shown; also cf. Bi and Poo, 1998; Feldman, 2000). The LTD timing window was assumed to be $0 > \Delta t > -75$ ms (Figure 2D).

For Model 1, all spike interactions were counted. For Model 2, only the interactions nearest to a postsynaptic spike were counted. Model 3 was based on Model 2, with the additional rule that a postsynaptic spike participating in an LTP interaction could not partake in an LTD pairing.

The two free parameters for LTP interactions (linear dependence on frequency, plus an intercept variable) were extracted by a multivariate two-dimensional weighted least-square fit to the averaged pre-before-post and post-before-pre frequency dependence data (Figures 1D and 7B, fit illustrated in Figure 8A). The average amount of residual depolarization (Figure 5D) was used when generating these fits.

The models were evaluated on the random firing data (Figure 8C). Traces from the induction of individual experiments were analyzed for spike positions, residual depolarization, and instantaneous postsynaptic frequency. The estimated change in synaptic strength was averaged across experiments before being compared to the corresponding averaged data points (Figure 8D). For both the weighted fits and the random firing predictions, the χ^2 (not shown) indicated the same relative goodness of fit as did the RMS.

Acknowledgments

We thank Alanna Watt, Larry Abbott, Mark van Rossum, Niraj Desai, Dan Feldman, Chris Hempel, and Nick Otmakhov for help and useful discussions, and Brynn Kessler, Ben Elgart, Stephanie Moore, and Mark Miller for assistance with histology. This work was supported by NIH grants EY11116 and MH58754, and the Sloan-Swartz Center for Theoretical Neurobiology.

Received May 17, 2001; revised October 26, 2001.

References

Abbott, L.F., and Nelson, S.B. (2000). Synaptic plasticity: taming the beast. Nat. Neurosci. *3*, 1178–1183.

Artola, A., Bröcher, S., and Singer, W. (1990). Different voltage-dependent thresholds for inducing long-term depression and long-term potentiation in slices of rat visual cortex. Nature *347*, 69–72.

Artola, A., and Singer, W. (1987). Long-term potentiation and NMDA receptors in rat visual cortex. Nature *330*, 649–652.

Barrionuevo, G., and Brown, T.H. (1983). Associative long-term potentiation in hippocampal slices. Proc. Natl. Acad. Sci. USA. *80*, 7347–7351.

Bekkers, J.M. (2000). Properties of voltage-gated potassium currents in nucleated patches from large layer 5 cortical pyramidal neurons of the rat. J. Physiol. *525 Pt 3*, 593–609.

Bi, G.Q., and Poo, M.M. (1998). Synaptic modifications in cultured hippocampal neurons: dependence on spike timing, synaptic strength, and postsynaptic cell type. J. Neurosci. *18*, 10464–10472.

Bienenstock, E.L., Cooper, L.N., and Munro, P.W. (1982). Theory for the development of neuron selectivity: orientation specificity and binocular interaction in visual cortex. J. Neurosci. *2*, 32–48.

Bliss, T.V., and Collingridge, G.L. (1993). A synaptic model of memory: long-term potentiation in the hippocampus. Nature *361*, 31–39.

Bliss, T.V., and Lømo, T. (1973). Long-lasting potentiation of synaptic transmission in the dentate area of the anaesthetized rabbit following stimulation of the perforant path. J. Physiol. (Lond.). *232*, 331–356.

Christie, B.R., Franks, K.M., Seamans, J.K., Saga, K., and Sejnowski, T.J. (2000). Synaptic plasticity in morphologically identified CA1 stratum radiatum interneurons and giant projection cells. Hippocampus *10*, 673–683.

Debanne, D., Gähwiler, B.H., and Thompson, S.M. (1994). Asynchronous pre- and postsynaptic activity induces associative long-term depression in area CA1 of the rat hippocampus in vitro. Proc. Natl. Acad. Sci. USA *91*, 1148–1152.

Debanne, D., Gähwiler, B.H., and Thompson, S.M. (1996). Cooperative interactions in the induction of long-term potentiation and depression of synaptic excitation between hippocampal CA3–CA1 cell pairs in vitro. Proc. Natl. Acad. Sci. USA *93*, 11225–11230.

Debanne, D., Gähwiler, B.H., and Thompson, S.M. (1998). Long-term synaptic plasticity between pairs of individual CA3 pyramidal cells

in rat hippocampal slice cultures. J. Physiol. (Lond.) *507 (Pt 1)*, 237–247.

Douglas, R.M., Goddard, G.V., and Riives, M. (1982). Inhibitory modulation of long-term potentiation: evidence for a postsynaptic locus of control. Brain Res. *240*, 259–272.

Dudek, S.M., and Bear, M.F. (1992). Homosynaptic long-term depression in area CA1 of hippocampus and effects of N-methyl-D-aspartate receptor blockade. Proc. Natl. Acad. Sci. U.S.A. *89*, 4363–4367.

Egger, V., Feldmeyer, D., and Sakmann, B. (1999). Coincidence detection and changes of synaptic efficacy in spiny stellate neurons in rat barrel cortex. Nat. Neurosci. *2*, 1098–1105.

Feldman, D.E. (2000). Timing-based LTP and LTD at vertical inputs to layer II/III pyramidal cells in rat barrel cortex. Neuron *27*, 45–56.

Finnerty, G.T., Roberts, L.S., and Connors, B.W. (1999). Sensory experience modifies the short-term dynamics of neocortical synapses. Nature *400*, 367–371.

Gerstner, W., Kempter, R., van Hemmen, J.L., and Wagner, H. (1996). A neuronal learning rule for sub-millisecond temporal coding. Nature *383*, 76–81.

Gray, C.M. (1999). The temporal correlation hypothesis of visual feature integration: still alive and well. Neuron *24*, 31–47, 111–125.

Gustafsson, B., Wigström, H., Abraham, W.C., and Huang, Y.Y. (1987). Long-term potentiation in the hippocampus using depolarizing current pulses as the conditioning stimulus to single volley synaptic potentials. J. Neurosci. *7*, 774–780.

Hoffman, D.A., Magee, J.C., Colbert, C.M., and Johnston, D. (1997). K^+ channel regulation of signal propagation in dendrites of hippocampal pyramidal neurons. Nature *387*, 869–875.

Kirkwood, A., and Bear, M.F. (1994). Hebbian synapses in visual cortex. J. Neurosci. *14*, 1634–1645.

Kirkwood, A., Dudek, S.M., Gold, J.T., Aizenman, C.D., and Bear, M.F. (1993). Common forms of synaptic plasticity in the hippocampus and neocortex in vitro. Science *260*, 1518–1521.

Koester, H.J., and Sakmann, B. (1998). Calcium dynamics in single spines during coincident pre- and postsynaptic activity depend on relative timing of back-propagating action potentials and subthreshold excitatory postsynaptic potentials. Proc. Natl. Acad. Sci. USA *95*, 9596–9601.

König, P., Engel, A.K., and Singer, W. (1996). Integrator or coincidence detector? The role of the cortical neuron revisited. Trends Neurosci. *19*, 130–137.

Korngreen, A., and Sakmann, B. (2000). Voltage-gated K^+ channels in layer 5 neocortical pyramidal neurones from young rats: subtypes and gradients. J. Physiol. *525*, 621–639.

Levy, W.B., and Steward, O. (1979). Synapses as associative memory elements in the hippocampal formation. Brain Res. *175*, 233–245.

Levy, W.B., and Steward, O. (1983). Temporal contiguity requirements for long-term associative potentiation/depression in the hippocampus. Neuroscience *8*, 791–797.

Liao, D., Jones, A., and Malinow, R. (1992). Direct measurement of quantal changes underlying long-term potentiation in CA1 hippocampus. Neuron *9*, 1089–1097.

Linsker, R. (1988). Self-Organization in a Perceptual Network. Computer *21*, 105–117.

Lisman, J. (1989). A mechanism for the Hebb and the anti-Hebb processes underlying learning and memory. Proc. Natl. Acad. Sci. USA *86*, 9574–9578.

Magee, J.C., and Johnston, D. (1997). A synaptically controlled, associative signal for Hebbian plasticity in hippocampal neurons. Science *275*, 209–213.

Malinow, R. (1991). Transmission between pairs of hippocampal slice neurons: quantal levels, oscillations, and LTP. Science *252*, 722–724.

Markram, H. (1997). A network of tufted layer 5 pyramidal neurons. Cereb. Cortex *7*, 523–533.

Markram, H., and Tsodyks, M. (1996). Redistribution of synaptic efficacy between neocortical pyramidal neurons. Nature *382*, 807–810.

Markram, H., Lübke, J., Frotscher, M., Roth, A., and Sakmann, B. (1997a). Physiology and anatomy of synaptic connections between thick tufted pyramidal neurones in the developing rat neocortex, J. Physiol. (Lond.) *500*, 409–440.

Markram, H., Lübke, J., Frotscher, M., and Sakmann, B. (1997b). Regulation of synaptic efficacy by coincidence of postsynaptic APs and EPSPs. Science *275*, 213–215.

McNaughton, B.L., Douglas, R.M., and Goddard, G.V. (1978). Synaptic enhancement in fascia dentata: cooperativity among coactive afferents. Brain Res. *157*, 277–293.

Migliore, M., Hoffman, D.A., Magee, J.C., and Johnston, D. (1999). Role of an A-type K^+ conductance in the back-propagation of action potentials in the dendrites of hippocampal pyramidal neurons. J. Comput. Neurosci. *7*, 5–15.

Miller, K.D. (1996). Synaptic economics: competition and cooperation in synaptic plasticity. Neuron *17*, 371–374.

Montgomery, J.M., Pavlidis, P., and Madison, D.V. (2001). Pair Recordings Reveal All-Silent Synaptic Connections and the Postsynaptic Expression of Long-Term Potentiation. Neuron *29*, 691–701.

Moore, C.I., and Nelson, S.B. (1998). Spatio-temporal subthreshold receptive fields in the vibrissa representation of rat primary somatosensory cortex. J. Neurophysiol. *80*, 2882–2892.

Mulkey, R.M., and Malenka, R.C. (1992). Mechanisms underlying induction of homosynaptic long-term depression in area CA1 of the hippocampus. Neuron *9*, 967–975.

Paré, D., Shink, E., Gaudreau, H., Destexhe, A., and Lang, E.J. (1998). Impact of spontaneous synaptic activity on the resting properties of cat neocortical pyramidal neurons in vivo. J. Neurophysiol. *79*, 1450–1460.

Perez, Y., Morin, F., and Lacaille, J.C. (2001). A hebbian form of long-term potentiation dependent on mGluR1a in hippocampal inhibitory interneurons. Proc. Natl. Acad. Sci. USA *98*, 9401–9406.

Pike, F.G., Meredith, R.M., Olding, A.W., and Paulsen, O. (1999). Rapid report: postsynaptic bursting is essential for "Hebbian" induction of associative long-term potentiation at excitatory synapses in rat hippocampus. J. Physiol. (Lond.). *518 (Pt 2)*, 571–576.

Schiller, J., Schiller, Y., and Clapham, D.E. (1998). NMDA receptors amplify calcium influx into dendritic spines during associative pre- and postsynaptic activation. Nat. Neurosci. *1*, 114–118.

Schiller, J., Major, G., Koester, H.J., and Schiller, Y. (2000). NMDA spikes in basal dendrites of cortical pyramidal neurons. Nature *404*, 285–289.

Senn, W., Markram, H., and Tsodyks, M. (2001). An algorithm for modifying neurotransmitter release probability based on pre- and postsynaptic spike timing. Neural Comput. *13*, 35–67.

Shadlen, M.N., and Newsome, W.T. (1998). The variable discharge of cortical neurons: implications for connectivity, computation, and information coding. J. Neurosci. *18*, 3870–3896.

Shadlen, M.N., and Movshon, J.A. (1999). Synchrony unbound: a critical evaluation of the temporal binding hypothesis. Neuron *24*, 67–77.

Song, S., Miller, K.D., and Abbott, L.F. (2000). Competitive Hebbian learning through spike-timing-dependent synaptic plasticity. Nat. Neurosci. *3*, 919–926.

Stuart, G.J., and Häusser, M. (2001). Dendritic coincidence detection of EPSPs and action potentials. Nat. Neurosci. *4*, 63–71.

Svoboda, K., Helmchen, F., Denk, W., and Tank, D.W. (1999). Spread of dendritic excitation in layer 2/3 pyramidal neurons in rat barrel cortex in vivo. Nat. Neurosci. *2*, 65–73.

Tsubokawa, H., and Ross, W.N. (1996). IPSPs modulate spike backpropagation and associated $[Ca2^+]i$ changes in the dendrites of hippocampal CA1 pyramidal neurons. J. Neurophysiol. *76*, 2896–2906.

Turrigiano, G.G. (1999). Homeostatic plasticity in neuronal networks: the more things change, the more they stay the same. Trends Neurosci. *22*, 221–227.

Turrigiano, G.G., Leslie, K.R., Desai, N.S., Rutherford, L.C., and Nelson, S.B. (1998). Activity-dependent scaling of quantal amplitude in neocortical neurons. Nature *391*, 892–896.

Turrigiano, G.G., and Nelson, S.B. (2000). Hebb and homeostasis in neuronal plasticity. Curr. Opin. Neurobiol. *10*, 358–364.

van Rossum, M.C.W., Bi, G.Q., and Turrigiano, G.G. (2000). Stable Hebbian Learning from Spike Timing-Dependent Plasticity. J. Neurosci. *20*, 8812–8821.

Vetter, P., Roth, A., and Häusser, M. (2001). Propagation of action potentials in dendrites depends on dendritic morphology. J. Neurophysiol. *85*, 926–937.

von der Malsburg, C. (1973). Self-organization of orientation-sensitive cells in striate cortex. Kybernetik *14*, 85–100.

Watt, A.J., van Rossum, M.C., MacLeod, K.M., Nelson, S.B., and Turrigiano, G.G. (2000). Activity coregulates quantal AMPA and NMDA currents at neocortical synapses. Neuron *26*, 659–670.

Wei, D.S., Mei, Y.A., Bagal, A., Kao, J.P., Thompson, S.M., and Tang, C.M. (2001). Compartmentalized and binary behavior of terminal dendrites in hippocampal pyramidal neurons. Science *293*, 2272–2275.

Yang, S.N., Tang, Y.G., and Zucker, R.S. (1999). Selective induction of LTP and LTD by postsynaptic [$Ca2^{+}$]i elevation. J. Neurophysiol. *81*, 781–787.

Yuste, R., and Denk, W. (1995). Dendritic spines as basic functional units of neuronal integration. Nature *375*, 682–684.

Zalutsky, R.A., and Nicoll, R.A. (1992). Mossy fiber long-term potentiation shows specificity but no apparent cooperativity. Neurosci. Lett. *138*, 193–197.

Zhang, L.I., Tao, H.W., Holt, C.E., Harris, W.A., and Poo, M. (1998). A critical window for cooperation and competition among developing retinotectal synapses. Nature *395*, 37–44.